Vehicle-Mounted Intelligent Surface for Cooperative Localization in Cellular Networks

Kaitao Meng*†, Qingqing Wu‡, Wen Chen‡, and Deshi Li§
*State Key Laboratory of Internet of Things for Smart City, University of Macau, Macau, China
†Department of Electrical and Electronic Engineering, University College London, London, UK
‡Department of Electronic Engineering, Shanghai Jiao Tong University, Shanghai, China
§Electronic Information School, Wuhan University, Wuhan, China
Emails: *kaitao.meng@ucl.ac.uk, ‡{qingqingwu, wenchen}@sjtu.edu.cn, §dsli@whu.edu.cn

***Abstract*—Due to the continuous increase in the communication frequency band of the sixth-generation (6G) wireless communication network, it can potentially provide positioning services for applications such as intelligent transportation. However, limited radar cross sections of vehicles may result in too weak echo signals and incorrect measurement associations, especially for base stations (BSs) with low transmit power. To tackle this issue, we propose a novel cooperative localization scheme in cellular networks, where the controllable signal reflection capabilities of intelligent reflecting surfaces (IRSs) are utilized to facilitate target association. Specifically, IRSs are mounted on the vehicles to enhance the echo signals towards the associated BS while reducing interference with other BSs. We aim to minimize the maximum Cramér-Rao lower bound (CRLB) of location errors by jointly optimizing target association, IRS phase shifts, and dwell time. However, solving this CRLB optimization problem is non-trivial due to the non-convex objective function. To this end, we transform the problem for single-vehicle localization into a monotonic optimization problem, thereby optimally solving it through the Polyblock-based algorithm. For multi-vehicle localization, we propose a heuristic algorithm to efficiently optimize the target association and dwell time allocation. Finally, our simulation results verify that deploying IRSs on vehicles can effectively improve the resolution ability of multi-vehicle positioning and reduce the BS number requirements.**

I. Introduction

In recent years, applications such as autonomous driving and intelligent transportation have brought a significantly increasing demand for high-accuracy and low-latency localization services for vehicles [1]. Benefiting from the continuous increase in the communication frequency band, cellular networks (CNs) are capable of providing sensing services, including range measurement, target detection and localization. Due to the widespread availability of CNs in cities, CN-based localization methods have the potential to provide seamless sensing coverage. In the literature, the majority of work on positioning through CNs focuses on the deployment of base stations (BSs), beamforming design, and allocation of resources [2].

Although the advantages mentioned above, achieving high-quality positioning based on CNs still faces crucial challenges. First, since receivers are unaware of concurrent reflections from multiple targets, it is difficult to match measurements with the right target, resulting in "ghost" targets, especially for dense-target scenarios [3]. Second, due to the random reflection coefficient and the generally small radar cross sections (RCS) of moving vehicles, the echo signals reflected from vehicles may be too weak for precise target detection/tracking [4]. Finally, when the trajectories of several targets are in close proximity to each other, conventional localization methods have difficulty in discriminating these targets. It is observed that these issues are primarily caused by the uncontrollability of echo signals. In fact, with the development of metamaterial technology, it is possible to control the propagation path of electromagnetic waves. Therefore, controlling echo signals become a promising solution to enhance localization performance and reduce interference to other devices.

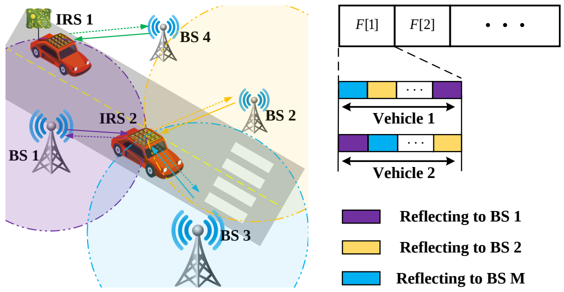

(a) Vehicular localization scenarios. (b) Localization protocol.

Fig. 1. Scenarios and protocol for IRS-assisted vehicle localization.

In addition to providing effective communication services, intelligent reflecting surfaces (IRSs) can also aid to sense targets in blind areas by establishing virtual light-of-sight (LoS) links between BSs and targets [5]. At present, the majority of existing works have focused on exploiting IRSs to improve sensing performance among static or low-mobility targets, where IRSs are generally deployed in fixed locations [6]. However, the coverage ability under such IRS deployment strategies may be constrained for high-mobility vehicles. How to achieve high-resolution and high-reliable localization as well as efficiently reduce interference between different measurements is still an open issue.

In this paper, we propose a novel cooperative localization scheme in WCNs, by employing IRSs on the surfaces of vehicles to facilitate their association between the measurement at the BSs, as shown in Fig. 1. In this way, the controllable signal reflection at the IRS sides can be exploited to enhance the reflected signal strength and reduce interference with unassociated devices. Then, in our considered system, the Cramér-Rao lower bound (CRLB) is adopted to describe the localization performance [7]. Due to the ability to actively control echo signals, the maximum CRLB of vehicles is minimized by jointly optimizing target association, IRS phase shifts, and dwell time, thereby ensuring the fairness of localization performance across multiple vehicles. To investigate the localization performance of the proposed sensing scheme, the maximum CRLB of vehicles is minimized by jointly optimizing target association, IRS phase shifts, and dwell time. However, solving this CRLB optimization problem is highly non-trivial due to the non-convex objective function and closely coupled variables. To tackle this issue, we prove the monotonicity of the CRLB with respect to (w.r.t.) the dwell time to facilitate solving the problem. The main contributions of this paper can be summarized as follows:

- We propose a novel IRS-aided cooperative localization scheme, where an IRS is mounted on the vehicle to enhance localization performance, and the beam flattening technique is presented to ensure sensing reliability.
- For single-vehicle localization, the problem is proved to be a monotonic optimization (MO) problem and can be optimally solved by the Polyblock-based algorithm. For multi-vehicle localization, we propose a heuristic algorithm to optimize the target association and time allocation effectively.
- Finally, our simulation results verify the effectiveness of the proposed cooperative localization scheme and validate its superiority over benchmark schemes.

II. System Model and Problem Formulation

As shown in Fig. 1, M cellular BSs with a single transmit antenna and a single receive antenna are employed to provide localization services for K vehicles. The targets can be extended to robots, unmanned aerial vehicles, etc. The BSs are indexed by $m \in \mathcal{M} = \{1, \cdots, M\}$, and the location of BS m is denoted by (x_m^r, y_m^r, H_m). The vehicles are indexed by $k \in \mathcal{K} = \{1, \cdots, K\}$, where an IRS is deployed on the surface of each vehicle for actively controlling echo signals. The target and IRS are interchangeable according to context in the following discussion. The uniform planar array (UPA) with half-wavelength antenna spacing is adopted at the IRS, and the number of IRS elements is $L = L_x \times L_y$, indexed by $l \in \mathcal{L} = \{1, \cdots, L\}$, where L_x and L_y denote the number of elements along the x- and y-axis, respectively.

A. Proposed Localization Scheme

To tackle the target association issues, we propose a novel cooperative localization scheme to actively control the direction of echo signals by designing the IRS phase shifts, and thus facilitate to establish the association between vehicles and the measured distances at the BSs, as shown in Fig. 1. It is practically assumed that the location of vehicles keeps constant within a sufficiently small time duration ΔT [8]. Then, the duration ΔT is further divided into several time slots, and the association between BSs and IRSs is optimized at different time slots. Specifically, the time duration ΔT is divided into N time slots, and N is optimized according to the numbers of vehicles and BSs, which will be discussed in Section IV. The time slots are indexed by $n \in \mathcal{N} = \{1, \cdots, N\}$ and the proportion of time slot n in ΔT is recorded as η_n with $\sum_{n=1}^{N} \eta_n = 1$. It is worth noting that the BSs do not need to interact with the vehicles, but only send control commands to the IRS controller to adjust the IRS phase shifts.

To establish a unique association between BSs and IRSs, we introduce the set of binary variables $\{b_{k,m,n}\}$, $k \in \mathcal{K}, m \in \mathcal{M}, n \in \mathcal{N}$, which indicates that BS m transmits signal $s_m(t)$, and then IRS k reflects incident signal $s_m(t)$ towards BS m for positioning vehicle k at time slot n if $b_{k,m,n} = 1$, otherwise, $b_{k,m,n} = 0$. To establish the unique association between measured distances and vehicles, at time slot n, the phase shifts of IRS k are designed to enhance the reflected echo signal power for at most one BS, i.e,

$$\sum\nolimits_{m=1}^{M} b_{k,m,n} \leq 1, \forall k \in \mathcal{K}, n \in \mathcal{N}. \quad (1)$$

Similarly, to avoid mutual interference between BSs and IRSs, at each time slot, each BS transmits signals to sense at most one vehicle, i.e.,

$$\sum\nolimits_{k=1}^{K} b_{k,m,n} \leq 1, \forall m \in \mathcal{M}, n \in \mathcal{N}. \quad (2)$$

Moreover, to simplify the practical implementation, we assume that one vehicle and one BS are associated at most one time slot as follows:

$$\sum\nolimits_{n=1}^{N} b_{k,m,n} \leq 1, \forall k \in \mathcal{K}, m \in \mathcal{M}. \quad (3)$$

By adopting the above constraints, the measured distance at the BSs can be associated with a certain vehicle, thereby effectively improving the localization accuracy and avoiding the complexity of target association.

Without loss of generality, the prior location of vehicle k, denoted by $(\hat{x}_k^t, \hat{y}_k^t)$, can be obtained based on its onboard sensors such as global positioning system (GPS) or the state estimation according to previous observations. Due to vehicle mobility or sensor measurement errors, the accurate 2D location of vehicle k, i.e., (x_k^t, y_k^t), is assumed to be uniformly distributed within a circle with the radius r_e and center point $(\tilde{x}_k^t, \tilde{y}_k^t)$, where $(\tilde{x}_k^t, \tilde{y}_k^t)$ represents the prior location of IRS k. For notational simplicity, vehicles are assumed to drive along a straight road that is parallel to the x-axis. At the nth time slot, the reflection-coefficient matrix of IRS k is given by $\mathbf{\Theta}_{k,n} = \mathrm{diag}(e^{j\theta_{k,1,n}}, ..., e^{j\theta_{k,L,n}})$, where $\theta_{k,l,n}$ denotes the reflecting phase shifts of the lth element of IRS k.

B. Radar Measurement Model

The low-pass equivalent of the signal transmitted from BS m is denoted by $s_m(t)$, and $\frac{1}{W}\int_{W\cdot\Delta t} |s_m(t)|^2 \, dt = 1$, where W is the number of symbols during signal processing interval and Δt is the time of one symbol. Following the assumption in [9], the transmitted signals are approximately orthogonal for any time delay τ of interest, i.e.,

$$\frac{1}{W}\int_{W\cdot\Delta t} s_m(t) s_{m'}^*(t-\tau) dt \approx \begin{cases} 1 & \text{if } m = m' \\ 0 & \text{if } m \neq m' \end{cases}, \quad (4)$$

where $(\cdot)^*$ denotes the conjugate operator. The vehicle k's direction relative to BS m is defined by $\{\varphi_{k,m}, \phi_{k,m}\}$, where $\varphi_{k,m}$ and $\phi_{k,m}$ respectively denote the azimuth and elevation angles of the geometric path connecting IRS k and BS m. The channel power gain between IRS k and BS m can be given by $\beta^G_{k,m} = \beta_0 d^{-2}_{k,m}$, where β_0 is the channel power gain at the reference distance 1 m. $\boldsymbol{h}^{\mathrm{DL}}_{k,m} \in \mathbb{C}^{1\times L}$ and $\boldsymbol{h}^{\mathrm{UL}}_{k,m} \in \mathbb{C}^{L\times 1}$ are respectively the downlink and uplink channel vectors between BS m and IRS k, given by $\boldsymbol{h}^{\mathrm{DL}}_{k,m} = \sqrt{\beta^G_{k,m}}\boldsymbol{a}_{\mathrm{IRS}}(\varphi_{k,m}, \phi_{k,m})$ and $\boldsymbol{h}^{\mathrm{UL}}_{k,m} = \sqrt{\beta^G_{k,m}}\boldsymbol{a}^T_{\mathrm{IRS}}(\varphi_{k,m}, \phi_{k,m})$, where $\boldsymbol{a}_{\mathrm{IRS}} = \left[1, \cdots, e^{-j\pi(L_x-1)\Phi_{k,m}}\right]^T \otimes \left[1, \cdots, e^{-j\pi(L_y-1)\Omega_{k,m}}\right]^T$, $\Phi_{k,m} = \sin(\phi_k)\cos(\varphi_k)$, $\Omega_{k,m} = \sin(\phi_k)\sin(\varphi_k)$, and $\otimes$ denotes the Kronecker product.

Let $\mu_{k,m}$ and $\tau_{k,m}$ respectively denote Doppler frequency and the round-trip delay of echo signals. At the nth time slot, the echo signals received at BS m can be expressed as

$$\begin{aligned} r_{m,n}(t) &= b_{k,m,n}\boldsymbol{G}_{k,m,n}\sqrt{P_{\mathrm{A}}}s_m(t-\tau_{k,m}) \\ &+ \sum\nolimits_{m'\neq m}^{M}\sum\nolimits_{k=1}^{K} b_{k,m',n}\boldsymbol{G}_{k,m',n}\sqrt{P_{\mathrm{A}}}s_{m'}(t-\tau_{k,m'}) \\ &+ b_{k,m,n}\sum\nolimits_{k'\neq k}^{K}\boldsymbol{G}_{k',m,n}\sqrt{P_{\mathrm{A}}}s_m(t-\tau_{k',m}) + z_m(t), \end{aligned} \tag{5}$$

where $\boldsymbol{G}_{k,m,n} = e^{j2\pi\mu_{k,m}t}\boldsymbol{h}^{\mathrm{UL}}_{k,m}\boldsymbol{\Theta}_{k,n}\boldsymbol{h}^{\mathrm{DL}}_{k,m}$. where P_{A} is the transmit power, $z_m(t) \in \mathcal{CN}(0, \sigma_s^2)$ represents the additive disturbance, and σ_s^2 is the noise power at the receive antennas of the BS. Note that the interference from other unassociated BSs can be removed by the filtering operations due to the orthogonality of signals in (4). The BS correlates the received signal with the associated normalized detection signal, and the signal-to-noise ratio (SNR) of the received echos reflected from IRS k is expressed in expectation form, i.e., $\gamma^{\mathrm{S}}_{k,m} = \sum_{n=1}^{N} b_{k,m,n}\frac{\eta_n\Delta T}{\Delta t}\frac{P_{\mathrm{A}}\mathbb{E}\left[\left|\boldsymbol{h}^{\mathrm{UL}}_{k,m}\boldsymbol{\Theta}_{k,n}\boldsymbol{h}^{\mathrm{DL}}_{k,m}\right|^2\right]}{P_{\mathrm{A}}\sum_{k'\neq k}^{K}\mathbb{E}\left[\left|\boldsymbol{h}^{\mathrm{UL}}_{k',m}\boldsymbol{\Theta}_{k',n}\boldsymbol{h}^{\mathrm{DL}}_{k',m}\right|^2\right]+\sigma_s^2}$, where $\frac{\Delta T}{\Delta t}$ represents the number of symbols during the time ΔT.

Based on the above analysis, by adopting a certain association $\{b_{k,m,n}\}$, the vector parameter $\boldsymbol{p}_k = [x^t_k, y^t_k]$ can be estimated based on the measured distance, e.g., least squares method and maximum likelihood estimation (MLE) method [10]. The estimated distance from BS m to IRS k is expressed as $\tilde{d}_{k,m} = d_{k,m} + z_{k,m}$, where the error of estimated distance $z_{k,m}$ is generally inversely proportional to the signal-to-noise ratio (SNR) of echo signals at the BS receiver [11], i.e.,

$$\sigma^2_{k,m} \propto (\gamma^{\mathrm{S}}_{k,m})^{-1}, \tag{6}$$

where $\gamma^{\mathrm{S}}_{k,m}$ is the SNR of the echo signal from target k at the receive antenna of BS m after match-filtering. Given a vector parameters $\boldsymbol{p}_k = [x^t_k, y^t_k]$, the unbiased estimate satisfies the following inequality

$$E_{\boldsymbol{p}_k}\left\{(\hat{\boldsymbol{p}}_k - \boldsymbol{p}_k)(\hat{\boldsymbol{p}}_k - \boldsymbol{p}_k)^T\right\} \geq \mathcal{I}^{-1}(\boldsymbol{p}_k), \tag{7}$$

where $\mathcal{I}(\boldsymbol{p}_k)$ is the Fisher Information matrix (FIM), and it can be obtained by utilizing the chain rule based on the measurement $\boldsymbol{d}_k = [d_{k,1}, \cdots, d_{k,M}]$, when the measurement noise is Gaussian and the distance measurement covariance matrix $\boldsymbol{\Sigma}_k$ is not dependent on the parameter $\boldsymbol{p}_k$, i.e.,

$$\mathcal{I}(\boldsymbol{p}_k) = \left(\nabla_{\boldsymbol{p}_k}\boldsymbol{d}(\boldsymbol{p}_k)\right)^T\boldsymbol{\Sigma}_k^{-1}\left(\nabla_{\boldsymbol{p}_k}\boldsymbol{d}(\boldsymbol{p}_k)\right), \tag{8}$$

where the distance measurement covariance matrix of M BSs is denoted by

$$\boldsymbol{\Sigma}_k = \begin{bmatrix} \sigma^2_{k,1} & \cdots & 0 \\ \vdots & \ddots & \vdots \\ 0 & \cdots & \sigma^2_{k,M} \end{bmatrix}_{M\times M}. \tag{9}$$

In (8), the Jacobian matrix $\nabla_{\boldsymbol{p}_k}\boldsymbol{d}(\boldsymbol{p}_k)$ is $\nabla_{\boldsymbol{p}_k}\boldsymbol{d}(\boldsymbol{p}_k) = \frac{\partial \boldsymbol{d}_k}{\partial \boldsymbol{p}_k}$, i.e., $\nabla_{\boldsymbol{p}_k}\boldsymbol{d}(\boldsymbol{p}_k) = \begin{bmatrix} \cos\varphi_{k,1}\cos\phi_{k,1} & \sin\varphi_{k,1}\cos\phi_{k,1} \\ \vdots & \vdots \\ \cos\varphi_{k,M}\cos\phi_{k,M} & \sin\varphi_{k,M}\cos\phi_{k,M} \end{bmatrix}$. The CRLB of vehicle k's location estimation error can be expressed as $\mathrm{CRLB}_k = \mathrm{tr}\left(\mathcal{I}^{-1}(\boldsymbol{p}_k)\right)$.

C. Problem Formulation

In this work, we aim to minimize the maximum CRLB of the location estimation error by jointly optimizing the BS-IRS association, the phase shift matrices of IRSs, and the time allocation. The problem is formulated as follows.

$$\begin{aligned} (\mathrm{P1}): \quad & \min_{\{\boldsymbol{\Theta}_{k,n}\},\boldsymbol{\eta},\{b_{k,m,n}\},N} \ \max_k \ \mathrm{CRLB}_k && (10) \\ \text{s.t.} \quad & (1)-(3), \\ & \theta_{k,l,n} \in [0, 2\pi), \forall k, l, n, && (10a) \\ & \sum\nolimits_{n=1}^{N}\eta_n = 1, && (10b) \\ & \eta_n \in [0,1], \forall n, && (10c) \\ & b_{k,m,n} \in \{0,1\}, \forall k, m, n, && (10d) \\ & N \in \mathbb{N}^+, && (10e) \end{aligned}$$

where $\boldsymbol{\eta} = [\eta_1, \cdots, \eta_N]$. Solving (P1) optimally is non-trivial due to the non-convex objective function, the closely coupled variables, and the uncertain number of time slots.

III. Single-Vehicle Localization

In this section, we consider the single-vehicle localization, i.e., $K = 1$, to draw useful insights into the IRS phase shift and time allocation design. Without loss of generality, the number of time slots is set to $N = M$, and then variables $\{b_{m,n}\}$ can be ignored since the association order has no effect on the CRLB value and the BS-IRS association can be recovered according to the time allocation results. For simplicity, the IRS is associated with the BSs in the order of the BS index. Then, (P1) is simplified to (by dropping the target index) minimizing the CRLB of the localization error, i.e.,

$$\begin{aligned} (\mathrm{P2}): \quad & \min_{\{\boldsymbol{\Theta}_m\},\boldsymbol{\eta}} \ \mathrm{CRLB} && (11) \\ \text{s.t.} \quad & \theta_{l,m} \in [0, 2\pi), \forall l, m, && (11a) \\ & \sum\nolimits_{m=1}^{M}\eta_m = 1, && (11b) \\ & \eta_m \in [0,1], \forall m. && (11c) \end{aligned}$$

In the following, we present a phase shift design method for robust localization, and derive a simpler expression of the CRLB w.r.t. time allocation $\boldsymbol{\eta}$.

A. Phase Shift Design for Robust Localization

In the considered system, we present the beam flattening technique to achieve efficient and robust localization [12]. Specifically, due to the uncertain location of the vehicle, spatial resolution angles from BS m to the IRS (i.e., Φ_m and Ω_m) lie within two angular spans, denoted by $\left[\bar{\Phi}_m, \underline{\Phi}_m\right]$ and $\left[\bar{\Omega}_m, \underline{\Omega}_m\right]$, where $\bar{\Phi}_m = \max_{x_m^t, y_m^t} \Phi_m$, $\underline{\Phi}_m = \min_{x_m^t, y_m^t} \Phi_m$, $\bar{\Omega}_m = \max_{x_m^t, y_m^t} \Omega_m$, and $\underline{\Omega}_m = \min_{x_m^t, y_m^t} \Omega_m$. By adopting beam flattening [12], when the IRS is associated with BS m, the IRS elements of each row along the x-axis are divided into Q_m^x sub-arrays with $L_x^s = L_x/Q_m^x$ elements in each sub-array. Similarly, the IRS elements of each column along the y-axis are divided into Q_m^y sub-arrays with $L_y^s = L_y/Q_m^y$ elements in each sub-array.

Here, the IRS phase shifts can be designed based on the beam flattening technique proposed in [12] and the BSs only need to transmit the angular span information to the IRS controller for phase shift design. Here, the details are omitted for brevity. By adopting beam flattening, even if the position of the vehicle is uncertain, the BS can always receive the echo signal reflected from the IRS. Then, the SNR of echo signals received at BS m can be recast in approximate form as

$$\gamma_m^S \approx \eta_m \bar{\gamma}_m^S, \tag{12}$$

where $\bar{\gamma}_m^S = \frac{\beta_0^2 \Delta T L^2}{Q_m^2 \Delta t d_m^4 \sigma_s^2}$ and $Q_m = Q_m^x Q_m^y$. According to (6), we have $\sigma_m^2 = \frac{C_0}{\gamma_m^S}$, where C_0 is the variance parameter of the estimation method. Let $\tilde{\gamma}_m = \bar{\gamma}_m \cos^2 \phi_m$, the CRLB of vehicle location estimation can be rewritten as

$$\tilde{\text{CRLB}} = \frac{C_0 \sum_{m=1}^{M} \eta_m \tilde{\gamma}_m}{\sum_{j=1}^{M-1} \eta_j \tilde{\gamma}_j \left(\sum_{i=j+1}^{M} \eta_i \tilde{\gamma}_i \sin^2(\varphi_i - \varphi_j)\right)}. \tag{13}$$

The simplified expression of CRLB in (13) shows that the sensing accuracy is only related to the azimuth difference between any two associated BSs to the vehicle, i.e., $\varphi_j - \varphi_i$, instead of the absolute azimuth angle. In this case, (P2) can be transformed as follows.

$$(\text{P2.1}): \quad \min_{\boldsymbol{\eta}} \quad \tilde{\text{CRLB}}, \quad \text{s.t.} \quad (11\text{b}), (11\text{c}). \tag{14}$$

B. Proposed Algorithm

For problem (P2.1), it is not difficult to verify that if $M = 1$, $\tilde{\text{CRLB}} \to \infty$. When there is prior knowledge about the region of the vehicle, two receivers ($M = 2$) would suffice for vehicle localization. When $M = 2$, it can be verified that the optimal time allocation $\eta_1^* = \frac{\sqrt{\tilde{\gamma}_2}}{\sqrt{\tilde{\gamma}_1} + \sqrt{\tilde{\gamma}_2}}$ and $\eta_2^* = \frac{\sqrt{\tilde{\gamma}_1}}{\sqrt{\tilde{\gamma}_1} + \sqrt{\tilde{\gamma}_2}}$.

Proposition 1: The CRLB value decreases monotonically as η_m increases.

Proof: Please refer to Appendix A. ■

Intuitively, the increase of the dwell time on any BS leads to the improvement of measurement accuracy, thereby improving the positioning accuracy of the vehicle. Lemma 1 implies that (P2.1) is an MO problem w.r.t. η_m, and thus (P2.1) can be optimally solved based on the framework of the Polyblock-based algorithm [13]. Specifically, during the rth iteration, the vector $\boldsymbol{\eta}^{(r)} = [\eta_1^{(r)}, \cdots, \eta_M^{(r)}]$ corresponding to the minimum $\tilde{\text{CRLB}}$ is selected, and then its projection point is calculated as $\eta_m^{(r)} = \frac{\eta_m^{(r-1)}}{\sum_{m=1}^{M} \eta_m^{(r-1)}}$. After each iteration, a smaller Polyblock set can be constructed by replacing the vertices $\boldsymbol{\eta}^{(r)}$ with the newly generated vectors. The algorithm details are omitted for brevity, more details refer to [13].

IV. Multi-Vehicle Localization

Similar to the adopted beam flattening technique for single-vehicle cases, if $b_{k,m,n} = 1$, the phase shift of IRS k is designed to cover the spatial span $\left[\bar{\Phi}_{k,m}, \underline{\Phi}_{k,m}\right]$ and $\left[\bar{\Omega}_{k,m}, \underline{\Omega}_{k,m}\right]$ along x- and y-axis, respectively. In this case, the echo signals will also be received by other BSs within this angular range relative to vehicle k, resulting in an uncertain association between vehicles and measured distances. To tackle this issue, the interference caused by unassociated IRS should be avoided according to the spatial relationship between IRSs and BSs. Here, the interference relationship can be described according to the prior location of vehicles. Specifically, if BSs m and IRS k are associated at a certain time slot, and the adopted beam flattening techniques (c.f. Section III) will cause interference to BS m' if $\left[\bar{\Phi}_{k,m}, \underline{\Phi}_{k,m}\right] \cap \Phi_{k,m'} \neq \emptyset$ and/or $\left[\bar{\Omega}_{k,m}, \underline{\Omega}_{k,m}\right] \cap \Omega_{k,m'} \neq \emptyset$, and in this case, let $w_{k,m,m'} = 1$; otherwise, $w_{k,m,m'} = 0$. Notice that if $b_{k,m,n} = 1$, BS m' should not work at the nth time slot if $w_{k,m,m'} = 1$. Based on the established interference graph $\{w_{k,m,m'}\}$, the interference can be avoided if the following constraints are satisfied, i.e.,

$$b_{k,m,n} + \sum\nolimits_{k' \neq k}^{K} b_{k',m',n} \leq 2 - w_{k,m,m'}, \forall k, m, n. \tag{15}$$

By satisfying the constraints in (15), the interference from unassociated IRS can be ignored due to the weak reflecting power outside the main lobe. Then, the SNR of the received echos can be expressed as

$$\gamma_{k,m}^{\text{S}} = \sum\nolimits_{n=1}^{N} b_{k,m,n} \eta_n \bar{\gamma}_{k,m}^S, \tag{16}$$

where $\bar{\gamma}_{k,m}^S = \frac{\beta_0^2 \Delta T L^2}{Q_{k,m}^2 \Delta t d_{k,m}^4 \sigma_s^2}$. Then, the CRLB of vehicle k can be approximated as

$$\tilde{\text{CRLB}}_k = \frac{C_0 \sum_{m=1}^{M} \bar{\gamma}_{k,m}^S \cos^2 \phi_{k,m}}{\sum_{j=1}^{M-1} \bar{\gamma}_{k,j}^S \cos^2 \phi_{k,j} (\sum_{i=j+1}^{M} \bar{\gamma}_{k,i}^S \cos^2 \phi_{k,i} \sin^2(\varphi_{k,i} - \varphi_{k,j}))}. \tag{17}$$

Thus, (P1) can be equivalently transformed into

$$(\text{P3}): \min_{\boldsymbol{\eta}, \{b_{k,m,n}\}, N} \quad \xi \tag{18}$$

$$\text{s.t.} \quad (10b) - (10e), (1) - (3),$$

$$\tilde{\text{CRLB}}_k \leq \xi, \forall k, \tag{18a}$$

$$b_{k,m,n} + \sum_{k' \neq k}^{M} b_{k',m',n} \leq 2 - w_{k,m,m'}, \forall k, m, n. \tag{18b}$$

Note that under the optimal association $\{b_{k,m,n}\}$, it can be readily verified that the optimal time allocation $\{\eta_m\}$ can be solved by the MO-based algorithm presented in Section III. Thus, a direct way to find the optimal solution to (P3)

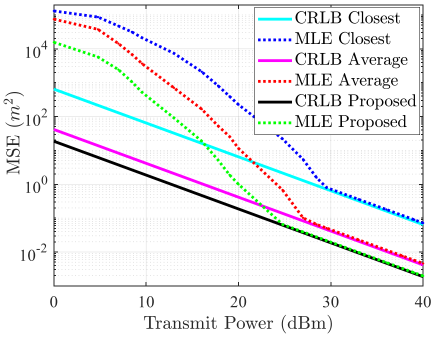

Fig. 2. MSE comparison versus CRLB under different transmit power.

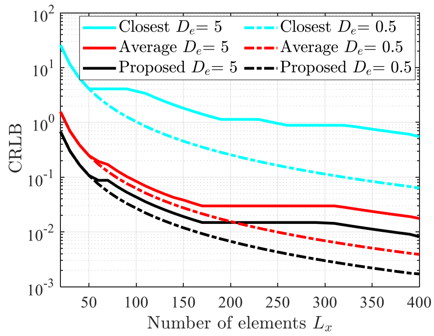

Fig. 3. Localization performance comparison versus different numbers of IRS elements.

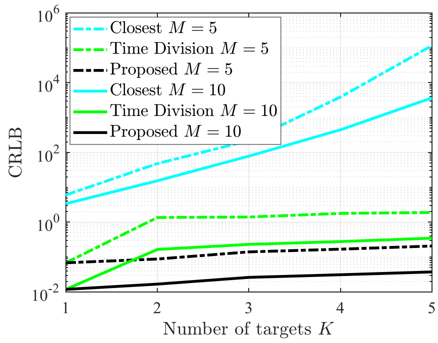

Fig. 4. statistical CRLB comparison versus different numbers of targets.

is to search all possible BS-IRS associations and calculate the corresponding optimal time allocation through the MO-based algorithm, and then the BS-IRS association with the minimum CRLB value is the optimal solution. However, such an operation is infeasible due to the high computational complexity, especially when the number of targets/BSs is large. To this end, we propose a heuristic BS-IRS association algorithm according to the derived conclusion in Section III.

According to the analysis in Section III, the sensing performance of the solution with only two BSs approaches to that of the optimal solution. Thus, we propose a two-step algorithm to solve target association and time allocation, where only two BSs with the minimum CRLB value are selected to localize each vehicle, thereby reducing the total number of time slots and the algorithm complexity. In this case, the total number of BS-IRS associations is $2K$, and the probability of potential interference is reduced. The associated BSs with IRS k are denoted by k_1 and k_2, and the optimal $\tilde{\text{CRLB}}_k^*$ is only affected by these two association time ratios, denoted by $\eta_{k,1}$ and $\eta_{k,2}$. Then, we normalize the CRLB of each vehicle, and the corresponding normalized time ratios can be denoted by $\bar{\eta}_{k,1} = \tilde{\text{CRLB}}_k^*\eta_{k,1}$ and $\bar{\eta}_{k,2} = \tilde{\text{CRLB}}_k^*\eta_{k,2}$, respectively. In this case, the obtained CRLB is the same for each vehicle using the normalized time ratio, thereby ensuring the fairness of multi-vehicle sensing. To make full use of space resources and achieve a better resource allocation effect, the BS-IRS associations are sorted according to the normalized time ratio, and then place these associations into the time slot set sequentially based on the interference-free graph $\{w_{k,m,m'}\}$. If the current BS-IRS association cannot be accommodated within the existing time slot set, a new time slot is generated, and $N \to N+1$. After updating the time slot, the BS-IRS associations are sorted based on the expected dwell time, thereby enhancing utilization efficiency of time resources.

V. Simulations

To validate our analysis and characterize the performance of the proposed localization scheme, Monte Carlo simulation results are presented in this section. The system parameters are given as follows: $L_x = L_y = 40$, $K = 10$, $M = 4$, $\beta_0 = -30$dB, $\sigma_s^2 = -80$dB, $P_{\text{A}} = 1$W, $D_e = 5$m, $\Delta T = 0.1$s, $\Delta t = 10^{-6}$s, and $C_0 = 0.1$. In addition, the following benchmark schemes are taken into account for comparison:

TABLE I
Statistics on the number of optimal associated BSs.

Number of associated BSs	2	3	4	5-10
Proportion	90%	8%	2%	0
Minimum value of $\{\eta_m\}$	0.29	0.018	0.001	-

- **Average**: The same time ratio is assigned to each BS.
- **Closest**: The two closest BSs to each vehicle are selected to be associated with the IRS.
- **Time Division**: Each vehicle is sensed on orthogonal time slots, with optimal time allocation separately.

First, the number of the associated BSs for the optimal solution is statistically analyzed by setting $M = 10$, as shown in Table I, where the location of BSs is randomly generated. It is worth noting that with probability 90%, the IRS only associates with two BS at the optimal solution, i.e., even if there are more candidate BSs, it tends to choose fewer BSs to associate with. This is expected since associating with more BSs will disperse the echo's energy, resulting in a decrease in the average accuracy of distance measurements. In other words, the diversity of measurement directions cannot compensate for the loss of distance measurement accuracy. Moreover, when the number of associated BSs increases, the minimum time ratio of the optimal solution gradually decreases. When the optimal number of associated BSs is 4, the minimum time ratio is only 0.001, which indicates the measurement of the corresponding BS is negligible.

Fig. 2 illustrates the performance for target localization in terms of the mean square error (MSE), with the increase of the transmit power P_{A}. The MLE method is adopted for obtaining the vehicle location via exhaustive grid search. As expected, the location MSEs of these schemes are lower-bounded by the corresponding CRLB, and the CRLB is tight and can be achieved by the MLE in the high-transmit power regime. It can be seen that the proposed method outperforms both benchmark scheme designs, especially when the transmit power is low. Compared to the 0.4/0.9 W transmit power's threshold to achieve a tight CRLB for the "average"/"closest" scheme, the proposed scheme can take the optimal time ratio to achieve that at a lower transmit power (i.e., 0.2 W) due to a better balance between different distance measurements.

In Fig. 3, the localization performance is compared under different numbers of IRS elements with $P_{\mathrm{A}} = 0.1$ W. The "average" scheme and the "closest" scheme lead to about 1.3 and 37.3 times higher CRLB as compared to the proposed scheme, respectively. Compared with $D_e = 0.5$ error bound of the vehicle's prior location, the CRLB gap between the case with $D_e = 0.5$ m and the case with $D_e = 5$ m becomes more pronounced with increasing the number of IRS elements L. The main reason is that the beam width of the echo signals becomes narrower with the increasing L, and thus the IRS needs to be divided into more sub-groups to ensure that the BS can receive echo signals effectively. The "closest" scheme with the prior location's error $D_e = 5$ achieves much worse positioning performance as compared to that of $D_e = 0.5$, which is mainly because the closer the potential distance between BS and IRS, the wider the beam should be designed to cover the potential angular range.

In Fig. 4, it can be observed that the CRLB of these considered schemes increases monotonically with the number of vehicles K, and the reduction of the CRLB achieved by our proposed scheme over two benchmark schemes increases as the number of vehicles increases. For each considered scheme, the CRLB with $M = 10$ can be reduced about 5 times compared to that with $M = 5$, and the main reason for the reduction in CRLB is that there are more BS-IRS associations with no interference to make sure more distances can be measured simultaneously. For the "closest" scheme, when the number of BSs is less (i.e., $M = 5$), the CRLB increases faster caused by potentially more severe interference and the reduced utilization efficiency of time resources. Notice that the proposed scheme is reduced to the "time division" scheme for single-vehicle cases, while for two-vehicle cases, the positioning performance of the "time division" scheme is severely degraded as compared to the proposed scheme. The main reason is that the interference probability between different BS-IRS associations is relatively low for less-vehicle cases, and the "time division" scheme does not fully utilize time and space resources.

VI. Conclusions

In this paper, we proposed a novel cooperative localization scheme with the active control of echo signals, where target association, IRS phase shifts, and dwell time are jointly optimized to improve sensing performance. For single-vehicle localization, we prove that the transformed problem is an MO, which can be optimally solved by the Polyblock-based algorithm. For multi-vehicle localization, a heuristic algorithm to optimize target association and time allocation. Finally, simulation results demonstrate that our proposed scheme achieves a significantly lower localization error over benchmark schemes.

Appendix A: Proof of Proposition 1

First, we let $x_m = \eta_m \bar{\gamma}_m^S \cos^2\phi_m$. Proposition 1 holds if CRLB is a monotonically decreasing function of x_m since x_m is an affine transformation of η_m. Let CRLB $\triangleq f(\boldsymbol{x}) = \frac{\sum_{m=1}^{M} x_m}{\sum_{m=1}^{M-1} x_m \sum_{i=m}^{M} x_i \sin^2(\phi_i - \sin\phi_m)}$, where $\boldsymbol{x} = [x_1, \cdots, x_M]$. The partial derivative of CRLB w.r.t. $x_{m'}$ can be given by

$$\frac{\partial f(\boldsymbol{x})}{\partial x_{m'}} = \frac{g(\boldsymbol{x})}{\left(\sum_{m=1}^{M-1} x_m \sum_{i=m}^{M} x_i \sin^2(\phi_i - \phi_m)\right)^2}, \qquad (19)$$

where $g(\boldsymbol{x}) = \sum_{m\neq m'}^{M-1} x_m \sum_{i\neq m,m'}^{M} x_i \sin^2(\phi_i - \phi_m) - \left(\sum_{m\neq m'}^{M} x_m\right) \sum_{i\neq m'}^{M} x_i \sin^2(\phi_i - \phi_m)$. In the following, it will be proved that for any given $\{\phi_m\}$, $\frac{\partial^2 f(\boldsymbol{x})}{\partial^2 x_{m'}} \leq 0$ always holds. Since $\frac{\partial^2 g(\boldsymbol{x})}{\partial^2 x_m} \leq 0$, we have $x_m^* = \arg\max_{x_m} g(\boldsymbol{x}) = 0$ if $\frac{\partial g(\boldsymbol{x})}{\partial x_m} \leq 0$. In this case, x_m can be removed. Otherwise, $\frac{\partial g(\boldsymbol{x})}{\partial x_m} > 0$, and the optimal solution to the maximum value of $g(\boldsymbol{x})$ is obtained if and only if $\frac{\partial g(\boldsymbol{x})}{\partial x_m} = 0$. Hence, we have $g(\boldsymbol{x}) = \sum_{m\neq m'}^{M} x_m (\sum_{i\neq m,m'}^{M} (\sin^2(\phi_m - \phi_{m'}) - \sin^2\phi_m - \sin^2\phi_{m'})) - (\sum_{m\neq m'}^{M} x_m^2 \sin^2(\phi_m)) \leq 0$. Thus, $\frac{\partial f(\boldsymbol{x})}{\partial x_m} \leq 0$, $\forall m \in \mathcal{M}$. The proof is completed.

VII. Acknowledgment

Q. Wu's work is supported by NSFC 62371289, Guangdong science and technology program under grant 2022A0505050011 and FDCT under Grant 0119/2020/A3.

References

[1] S. Gyawali, S. Xu, Y. Qian, and R. Q. Hu, "Challenges and solutions for cellular based V2X communications," *IEEE Commun. Surveys Tuts.*, vol. 23, no. 1, pp. 222–255, 1st Quart. 2021.

[2] Q. Shi, L. Liu, S. Zhang, and S. Cui, "Device-free sensing in OFDM cellular network," *IEEE J. Sel. Areas Commun.*, vol. 40, no. 6, pp. 1838–1853, Jun. 2022.

[3] J. Bosse, O. Krasnov, and A. Yarovoy, "Direct target localization and deghosting in active radar network," *IEEE Trans. Aerosp. Electron. Syst.*, vol. 51, no. 4, pp. 3139–3150, Oct. 2015.

[4] K. Meng *et al.*, "Intelligent surface empowered sensing and communication: A novel mutual assistance design," *IEEE Commun. Lett.*, 2023.

[5] ——, "Intelligent reflecting surface enabled multi-target sensing," *IEEE Trans. Commun.*, vol. 70, no. 12, pp. 8313–8330, Dec. 2022.

[6] X. Mu *et al.*, "Simultaneously transmitting and reflecting (STAR) RIS aided wireless communications," *IEEE Trans. Wireless Commun.*, vol. 21, no. 5, pp. 3083–3098, May 2022.

[7] J. Li *et al.*, "Range compression and waveform optimization for MIMO radar: A cramér–rao bound based study," *IEEE Trans. Signal Process.*, vol. 56, no. 1, pp. 218–232, 2008.

[8] S. Jayaprakasam, X. Ma, J. W. Choi, and S. Kim, "Robust beam-tracking for mmWave mobile communications," *IEEE Commun. Lett.*, vol. 21, no. 12, pp. 2654–2657, Dec. 2017.

[9] H. Godrich, A. M. Haimovich, and R. S. Blum, "Target localization accuracy gain in MIMO radar-based systems," *IEEE Trans. Inf. Theory*, vol. 56, no. 6, pp. 2783–2803, Jun. 2010.

[10] I. J. Myung, "Tutorial on maximum likelihood estimation," *J. Math. Psychol.*, vol. 47, no. 1, pp. 90–100, 2003.

[11] A. Liu *et al.*, "A survey on fundamental limits of integrated sensing and communication," *IEEE Commun. Surveys Tuts.*, vol. 24, no. 2, pp. 994–1034, 2nd Quart. 2022.

[12] H. Lu *et al.*, "Aerial intelligent reflecting surface: Joint placement and passive beamforming design with 3D beam flattening," *IEEE Trans. Wireless Commun.*, vol. 20, no. 7, pp. 4128–4143, Jul. 2021.

[13] Y. J. Zhang, L. P. Qian, and J. Huang, "Monotonic optimization in communication and networking systems," *Found. Trends Netw.*, vol. 7, no. 1, pp. 1–75, Oct. 2013.